Preparation of Ti/Al composite plates by differential temperature rolling with induction heating

Chao Yu
National Engineering Research Center for Equipment and Technology of Cold Rolled Strip
zhibin He (zb.ho@foxmail.com)
Yanshan University https://orcid.org/0000-0002-9432-9215
Qiang Lv
National Engineering Research Center for Equipment and Technology of Cold Rolled Strip
Jirui Yu
National Engineering Research Center for Equipment and Technology of Cold Rolled Strip
Hong Xiao
National Engineering Research Center for Equipment and Technology of Cold Rolled Strip

Research Article

Keywords: Ti/Al composite plate, Electromagnetic heating, Differential temperature rolling, Interfacial bonding strength, Homogeneous deformation

Posted Date: April 19th, 2021

DOI: https://doi.org/10.21203/rs.3.rs-424526/v1

Version of Record: A version of this preprint was published at The International Journal of Advanced Manufacturing Technology on July 29th, 2021. See the published version at https://doi.org/10.1007/s00170-021-07775-z.

Preparation of Ti/Al composite plates by differential temperature rolling with induction heating

Chao Yu, Zhibin He, Qiang Lv, Jirui Yu, Hong Xiao*

National Engineering Research Center for Equipment and Technology of Cold Rolled Strip, Qinhuangdao, 066004

*Corresponding author.

E-mail address: xhh@ysu.edu.cn (H. Xiao)

Abstract: In the current study, we proposed a method of differential temperature rolling with electromagnetic induction heating to prepare Ti/Al composite plates in a protective atmosphere to realize the homogeneous deformation of Ti/Al bonding rolling and improve the interfacial bonding strength of the composite plates. The temperature field required for homogeneous deformation rolling of titanium and aluminum was constructed through finite element simulation by adjusting the parameters of electromagnetic induction heating, which made a temperature difference of about 632 °C between titanium and aluminum, and the temperature of each plate was relatively uniform. The induction heating experiment was designed based on the finite element simulation, and the accuracy of the simulation results was verified by the experiment. The effects of rolling temperature and reduction rate of homogeneous deformation and bonding strength of Ti/Al composite plates were studied by rolling experiments. When the heating temperature of the Ti plate is 750-850 °C, and the reduction rate is 30%-48%, with the increase of rolling temperature and reduction rate of titanium, the reduction rate of Ti plate and Al plate gradually tend to be the same. When the temperature of titanium plate and aluminum plate is 850 °C and 188 °C, respectively, with the rolling reduction rate of 48%, the deformation rate of Ti plate and Al plate is 46.8% and 48.6%, respectively, and the bonding strength of the composite plate reaches 77MPa.

Keywords: Ti/Al composite plate; Electromagnetic heating; Differential temperature rolling; Interfacial bonding strength; Homogeneous deformation.

0 Introduction

Titanium, "space metal", with excellent properties such as high strength, low density, corrosion resistance, and fatigue resistance, is widely used in aerospace, military, and medical fields [1-3]. Aluminum has a broad application in various industrial fields due to its optimum electrical and thermal conductivity, corrosion resistance, and low price [4]. However, the high price of titanium limited its application. The performance of aluminum at high temperature and the corrosive environment is greatly reduced. The Ti/Al composite plate has "complementary effect", maintaining the characteristics of Ti and Al, which can obtain excellent comprehensive performance and significantly reduce the operating cost after proper combination [5]. Ti/Al composite has a broader application prospect in aerospace, metallurgical machinery, petrochemical industry, and other fields [6-8].

The main preparation methods of Ti/Al composite plate include explosive welding [9], solid-liquid cast-roll bonding [10] and roll bonding, etc. [11]. Fan [12] successfully prepared Ti/Al/Ti composite laminates by explosive welding using rock powder emulsion explosives and

studied the interface characteristics and bonding properties. However, the explosion produces seismic waves, noise, and toxic gases during preparation, which goes against the trend of green development of the modern industry. Huang [10] prepared Ti/Al composite plates by solid-liquid cast-rolling bonding and analyzed the mechanical properties and interfacial microstructure. The challenges, including heat transfer and flow in the solid-liquid cast-rolling bonding process, control casting temperature, and cast-rolling speed still demand prompt solution. Compared with explosive welding and solid-liquid cast-rolling bonding, roll bonding has many advantages, including high dimensional accuracy of the product, uniform thickness of each plate of composite material, uniformity and consistent properties of composite material, high production continuity, which is conducive to the realization of mass production and automation [13, 14].

Currently, there are two main problems in the process of rolling Ti/Al composite plates. First, the strength of the composite plate is on the low side. Second, due to the large difference in deformation resistance between titanium and aluminum metals, the deformation of the composite plate is not homogeneous, the plate warps, and the plate thickness ratio after rolling is difficult to control [15]. Peng [16] prepared Ti/Al composite plates by cold rolling and annealed at 515 °C×12 h, and the bonding strength reached the maximum of 40MPa; however, with the increasing annealing time, the interfacial bonding strength decreased. Ma [17] found that the deformation coordination between titanium and aluminum metal became worse with the increase of heating temperature during the preparation of Al/Ti/Al laminated plates by hot rolling. To solve the inhomogeneous deformation of Ti/Al rolling, Xiao [18] stacked titanium plates heated separately to 800 °C with aluminum plates of room-temperature and rolled them together, which improved the coordination of deformation of titanium and aluminum in the differential temperature state. The titanium plate needs to be placed on the steel plate and heated together, because the titanium plate is thin and heat dissipation is fast. From the furnace to the rolling, the steel plate can transfer heat and thermal insulation on the titanium plate. The operation of this method is complicated, and the surface of the titanium plate is highly oxidized, and the thickness of the oxide layer reaches 5 μm. Based on this, Qi [19] adopted the stacking order of slab of "Al/Ti/separators/pure iron/separators/Ti/Al", and made the aluminum and titanium to form a temperature difference of 305 °C through heat transfer of pure iron plate. They utilized the characteristic that pure iron can be heated to Curie point 770 °C rapidly in the alternating magnetic field due to the magnetic agglomeration effect, reducing the deformation resistance difference between titanium and aluminum. The rolled plates are separated from the separator, and two Ti/Al composite plates are obtained. However, the complicated assembly pattern will waste the pure iron plate, which is not conducive to industrial production.

The Ti/Al blank was heated by an electromagnetic induction coil in this paper. A large temperature difference of the titanium and aluminum was formed by selecting the suitable electromagnetic induction heating parameters, realizing the coordinative deformation of Ti/Al differential temperature rolling composite. This method is simple and easy to operate, which is beneficial to industrial production.

1 Simulation of induction heating before rolling and experiment

1.1 Induction heating model of the combined slab

Maxwell equations are used to solve the electromagnetic field problems in finite element analysis, and the expression is shown in Equation (1).

$$\left.\begin{aligned} \nabla \cdot D &= \rho \\ \nabla \times E &= -\frac{\partial B}{\partial t} \\ \nabla \cdot B &= 0 \\ \nabla \times H &= j + \frac{\partial D}{\partial t} \end{aligned}\right\} \tag{1}$$

In this equation, ∇ is Laplace operator; D is the electric flux density, $C \cdot m^{-2}$; ρ is charge density , $C \cdot m^{-3}$; E is electric field intensity, $V \cdot m^{-1}$; B is magnetic induction intensity, $Wb \cdot m^{-2}$; H is magnetic field intensity, $A \cdot m^{-1}$; j is the vector of the density of current, and $A \cdot m^{-2}$; t is time, s。

The eddy generated by electromagnetic induction is used as an internal heat source to increase the temperature of the slab. The equation for the intensity of internal heat source is as follows:

$$q_v = \frac{|j|^2}{\sigma} \tag{2}$$

In this equation：q_v is the intensity of internal heat source, $W \cdot m^{-3}$; σ is conductivity, $S \cdot m^{-1}$.

Assuming that the slab material is isotropic, the differential equation of the thermal conductivity during slab induction heating is shown in Equation (3).

$$\frac{\partial^2 T}{\partial x^2} + \frac{\partial^2 T}{\partial y^2} + \frac{\partial^2 T}{\partial z^2} + \frac{q_v}{k} = \frac{\rho c}{k} \cdot \frac{\partial T}{\partial \tau} \tag{3}$$

In this equation, T is time, K; k is the thermal conductivity, $W \cdot (m \cdot K)^{-1}$; ρ is density, $kg \cdot m^{-3}$; c is specific heat capacity, $W \cdot (kg \cdot K)^{-1}$。

Thermal convection and thermal radiation are the main reasons for heat loss of workpiece in the process of solving the temperature field, and the boundary conditions of the workpiece temperature field are shown in Equation (4).

$$k\left(\frac{\partial T}{\partial x} n_x + \frac{\partial T}{\partial y} n_y + \frac{\partial T}{\partial z} n_z\right) = a_c (T_a - T_s) + a_r (T_a - T_s) \tag{4}$$

In this equation, n_x、n_y、and n_z are direction vectors in three-dimensional space respectively; a_c is the coefficient of thermal convection, $W \cdot (m^2 \cdot K)^{-1}$; a_r is the coefficient of thermal radiation, $W \cdot (m^2 \cdot K)^{-1}$; T_a、 and T_s are ambient temperature and temperature of workpiece surface respectively, K.

The longitudinal magnetic induction heating efficiency is reduced when heating non-ferromagnetic metals, and the slab cannot even be heated to the specified temperature. The transverse magnetic induction heating was adopted in this paper. The magnetic force line of the transverse induction heating is perpendicular to the surface of the slab, and the eddy current distribution is approximate to the projection of the coil on the workpiece. The magnetic flux line of the sheet magnetic field could be redistributed by using a magnetizer piece [20]. The rectangular induction heating coil is established according to the shape of the slab, and the

magnetizer is placed in the middle of the coil to increase the magnetic gathering ability, increasing the heating temperature in the central zone of the slab.

Fig. 1a shows the slab combination, in which 1mm thick aluminum shims are placed between the titanium plate and the aluminum plate to reduce the heat transfer from the titanium plate to the aluminum plate. Fig. 1b shows the induction heating model, and the induction heating parameters are shown in Table 1. Considering the influence of the skin effect, the mesh was refined at the edge of the workpiece to ensure the accuracy of the calculation. The temperature-related material parameters of TA1 and 6061 are shown in Table 2.

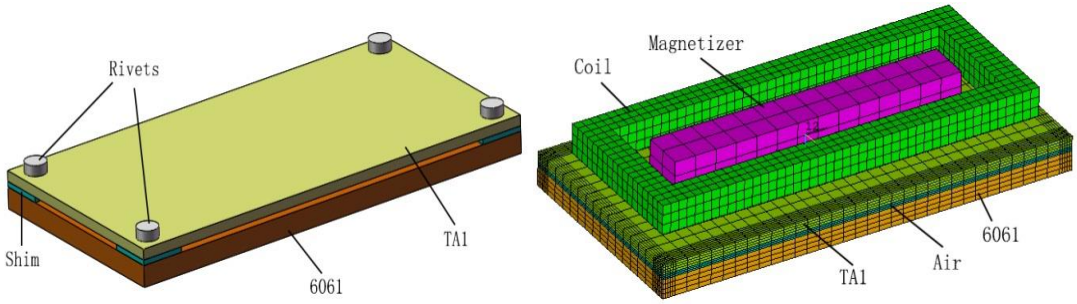

(a) Schematic diagram of assemble pattern (b) Schematic diagram of induction heating model.

Fig. 1 Induction heating model

Table 1 Main parameters of induction heating coil

parameters	values	parameters	values
Size of TA1 /mm	100×50×2	Size of coil/mm	92×36×6
Size of 6061/mm	100×50×4	Area of coil/mm	6×6
Size of magnetizer/mm	80×10×8	Clearance between coil and titanium plate/mm	3
Current frequency/Hz	76000	electric current density/(A/m^2)	2.4×10^7

Table 2 Material properties

Material	Temperature (°C)	electrical resistivity (×10^{-7}Ω·m)	coefficient of heat conduction (W·(m·K)$^{-1}$)	specific heat capacity (W·(kg·K)$^{-1}$)
TA1	600	14	19.4	591
	700	14.2	19.55	633
	800	14.4	19.7	654
	900	14.8	20.7	675
6061	20	0.27	176	960
	100	0.39	180	963
	200	0.45	184	1005
	300	0.6	188	1047

The finite element software ANSYS was used to performed the calculation using the sequential coupling method. The calculation results of the electromagnetic field were taken as the load of the temperature field to realize the electromagnetic-thermal coupling analysis. The flow

chart is shown in Figure 2.

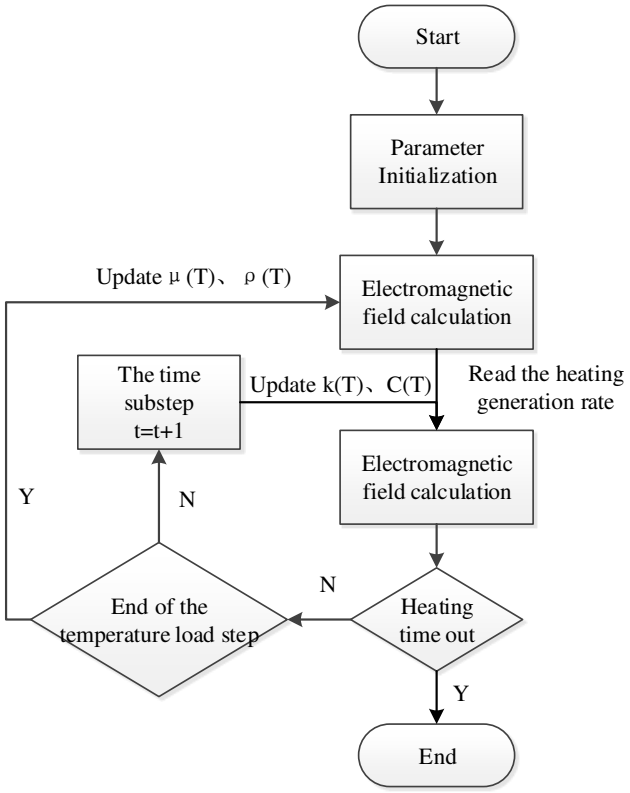

Fig. 2 Flow chart of induction heating by finite element simulation

1.2 Design of induction heating experiment

The experimental device was designed according to the parameters of the finite element model. Fig. 3 4 are respectively the schematic diagram of the composite process and actual process diagram of Ti/Al induction heating and differential temperature rolling. Induction heating equipment is mainly composed of a transverse magnetic coil, cooling system, and electronic control system. The composite slab from the top of the induction coil was pushed into the mill with a push rod immediately to get rolled in different temperature when the process of heating finished, which realized the whole process of sealing and argon gas protection from heating to rolling, prevent the oxidation on the surface of the plate while heating.

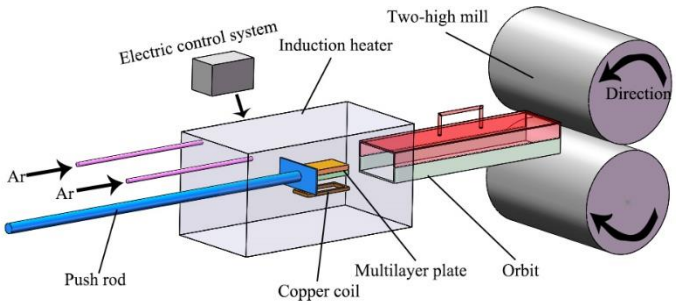

Fig. 3 Schematic diagram of differential temperature rolling with induction heating method

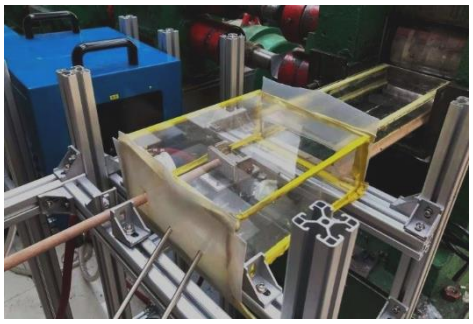

Fig. 4 Experimental platform

The experimental materials were commercial-purified titanium TA1 and AA 6061 aluminum alloy, and the sizes of the sheet are shown in Table 1. In the experiment, dirt and oxides on the surfaces of plates were cleared by a grinding machine equipped with 180 grit SiC paper, then the surfaces were cleaned with acetone and alcohol repeatedly to remove the grease stains on them and blown dry with a hairdryer. The slab was assembled as shown in Fig. 1a. Shims with a thickness of 1mm were placed between the titanium plates and aluminum plates. Finally, four ends of the slabs were fixed with aluminum rivets. A thermocouple thermometer and thermal infrared camera were used to record the temperature variation of the slab in the induction heating experiment. A hole with a diameter of 1mm and a depth of 10mm was drilled on both sides of the TA1 and AA 6061. Then, one end of the thermocouple (K-type) was inserted into the hole, and the other end was connected to the thermometer to record the temperature change of the slab. The surface of the titanium plate was photographed with the infrared thermal camera to record its temperature distribution.

Table 3 Chemical composition of TA1 (mass fraction, %)

Fe	Si	C	N	H	O	Ti
0.15	0.1	0.05	0.03	0.015	0.15	Bal.

Table 4 Chemical composition of AA6061 (mass fraction, %)

Cu	Si	Mg	Zn	Mn	Cr	Fe	Ti	Al
0.15	0.6	1.2	0.25	0.15	0.2	0.7	0.15	Bal.

1.3 Results of simulation and experiment

Figure 5 shows the comparison between the slab temperature recorded by thermocouple and the simulation. During the heating time of 25s from the beginning, the simulated and experimental slab temperatures are basically consistent. The heat loss of the titanium plate increases with the increase in titanium plate temperature; therefore, the warming trend of the titanium plate gradually slows down. The heat transfer from titanium plate to aluminum plate increases gradually, leading to a faster temperature rise of aluminum plate, and the temperature difference between titanium and aluminum first increases and then decreased. When induction heating lasted for 24s, the temperature of the titanium plate was 850 °C, and that of the aluminum plate was 188 °C, and the deformation resistance difference between the two metals was significantly reduced. At this time, the required temperature field of the Ti/Al differential temperature rolling was successfully

constructed.

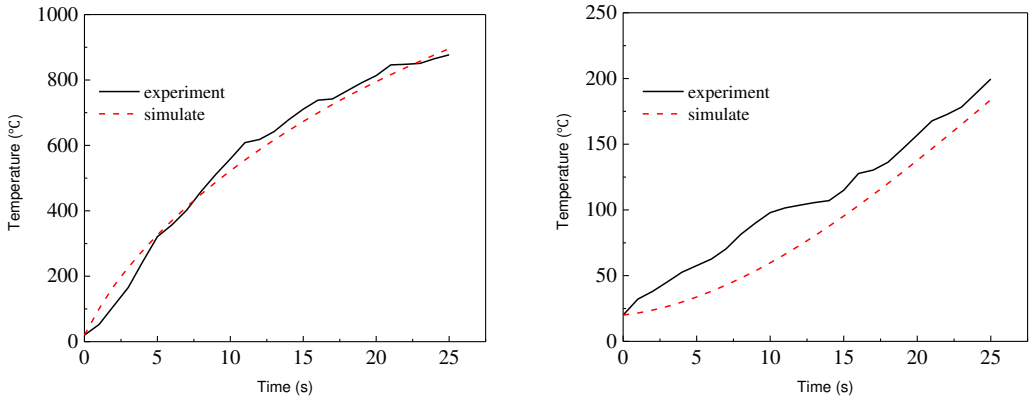

(a) Temperature of Ti plate

(b) Temperature of Al plate.

Fig. 5 Temperature variation of the slab

Setting the heating time as 24s, Fig. 6a and b) show the cloud picture of the simulated slab temperature distribution and the diagram of the slab temperature distribution taken by the experimental thermal camera. Comparing Fig. 6a with Fig. 6b, it can be seen that the surface temperature distribution of simulated and experimental titanium plates is consistent. Temperature distribution of titanium plates ranges from 700 °C to 911 °C, and that of aluminum plates ranges from 171-177 °C, meeting the requirements Ti/Al differential temperature rolling.

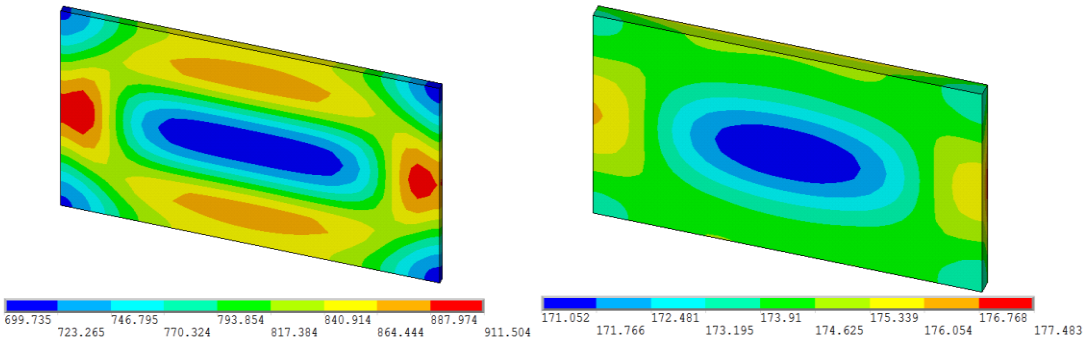

(a) cloud picture of the simulated Ti plate temperature

(b) cloud picture of the simulated Al plate temperature

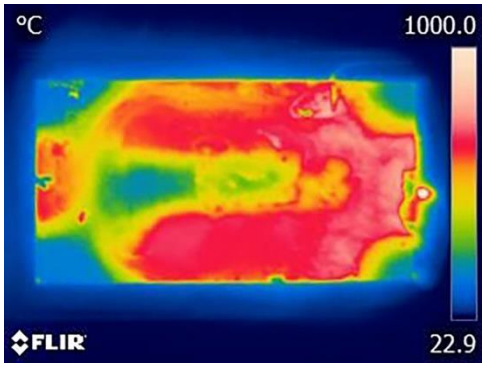

(c) cloud picture of the experimental Ti plate temperature distribution

Fig. 6 Cloud picture of slab temperature distribution

To study the temperature inhomogeneity in the transverse direction of the heated slab, the cross-sections at the front and middle positions of the slab were taken as the research objects, as shown in Fig. 7. The temperature distribution of the cross-sections, as well as the temperature

distribution and changes on the paths AB and MN were analyzed.

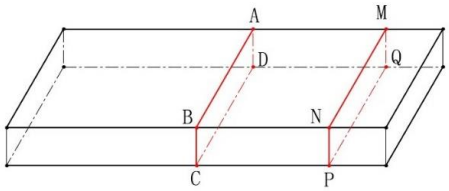

Fig. 7 Position picture of the selected point of the slab

Fig. 8 shows the temperature distribution of the cross-section of aluminum plate and titanium plate under heating induction for 24s. As can be seen from Fig. 8a and b , on the two sections, the temperature distribution along the thickness and width directions of the aluminum plate is homogeneous, and the temperature difference is less than 6 °C. However, the temperature distribution of the titanium plate is homogeneous along the thickness direction only. In the width direction, the fringe temperature of the titanium plate is 182 °C, higher than the central temperature at the interface of ABCD. At the MNPQ section, the fringe temperature of the plate is about 131 °C lower than the central part. Where the fringe temperature of titanium plate is high, the magnetic field and current effect are the strongest. In the middle part, the magnetic field is weak, and the efficiency of heating is low. Moreover, the slow heat transfer rate of titanium leads to the inhomogeneous temperature distribution of titanium plate. The heat transfer rate of the aluminum plate is more than five times of titanium, so the temperature distribution of the aluminum plate is homogeneous. In production, the billet is long, and mobile induction heating is generally adopted. When the billet passes through different positions of the coil, the heating effect of the fringe and the middle position is complementary. Consequently, the billet can be heated more evenly along the width direction.

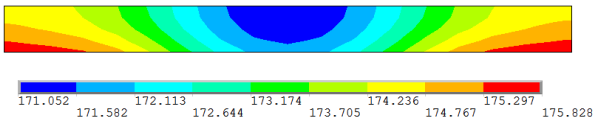

(a) Al plate cross-section of ABCD

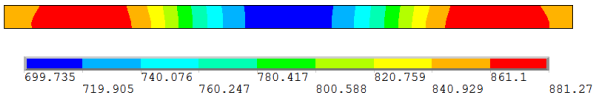

(b) Ti plate cross-section of ABCD

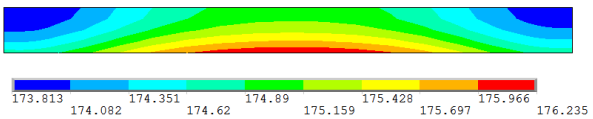

(c) Al plate cross-section of MNPQ

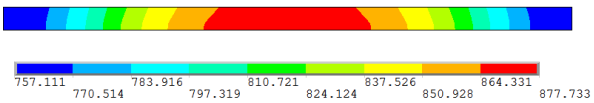

(d) Ti plate cross-section of MNPQ

Fig. 8 Temperature field of slab cross-section

2 Differential temperature composite rolling experiment and result

To compare the influence of rolling temperature on the composite plate property, we selected heating times as 18s, 21s, and 24s. At these times, the central temperature of the titanium plate was about 750 °C, 800 °C and 850 °C. The differential temperature composite rolling experiment was conducted under different reduction rates with a roll diameter of 200 mm and a rolling speed of 50 mm/s.

In this experiment, six shear specimens were cut from each composite plate parallel to the rolling direction, and the tensile-shear test was performed using an INSPEKT Table 100kN instrument with the test speed of 1mm/min. Then the average of the six results was obtained as the shear strength of the composite plate. The diagram of tensile-shear specimens is shown in Fig. 9. Metallographic specimens for observation were extracted along the rolling direction. The specimens were gradually burnished to No.3000 using emery papers from low particle size to high particle size, and then polished with SiO2 suspensions. Ti/Al composite plates morphology of the nearby bonding interface and the tensile-shear fracture microstructure were observed via a scanning electron microscope (SEM), and the adjacent combining interface and element distribution of the shear fracture were analysed using an energy dispersive spectrometer (EDS).

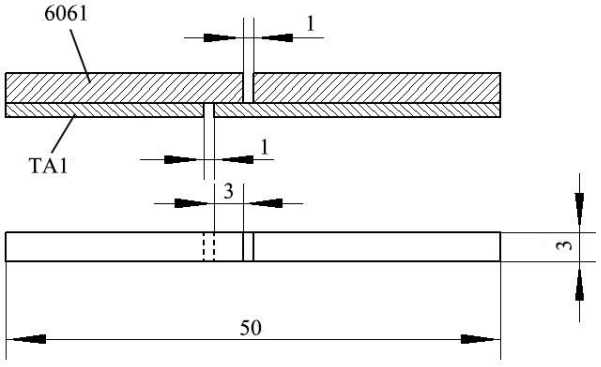

Fig. 9 Tensile-shear specimen diagram

The thickness of each plate of Ti/Al composite plate was measured via an optical microscope, and the metal deformation ratio of each plate is shown in Fig. 10. It can be seen that with the increase of rolling temperature, the deformation ratio of titanium and aluminum and the rolling reduction ratio of composite plate tend to be close. It shows that with the increase of the titanium plate temperature, the difference of deformation resistance between titanium and aluminum metal becomes smaller, and the deformation of the Ti/Al composite plate tends to be homogeneous. Therefore, increasing the rolling temperature of the titanium plate appropriately is conducive to the homogeneous deformation of the composite plate. As can be seen from Figure 11, when the rolling temperature of titanium plate is 850 °C, with the increase of the overall reduction of laminated composite, the deformation amount of both metals tends to be consistent, and the homogeneity of deformation is improved to a certain extent. When the reduction is 48%, the deformation of the titanium plate is 46.8%, and that of the aluminum plate is 48.6%. Therefore, increasing the rolling reduction appropriately is conducive to the homogeneous deformation of titanium and aluminum.

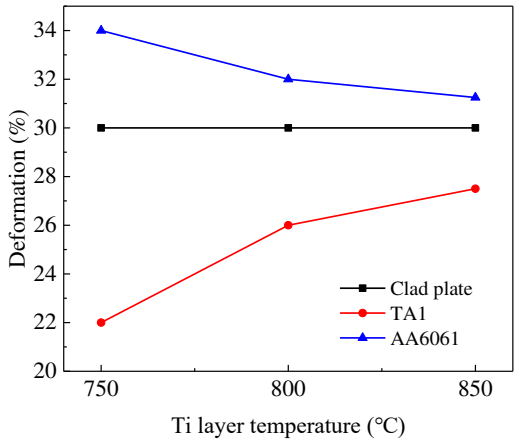

Fig. 10 Deformation rate of Ti and Al with 30% reduction at different temperatures

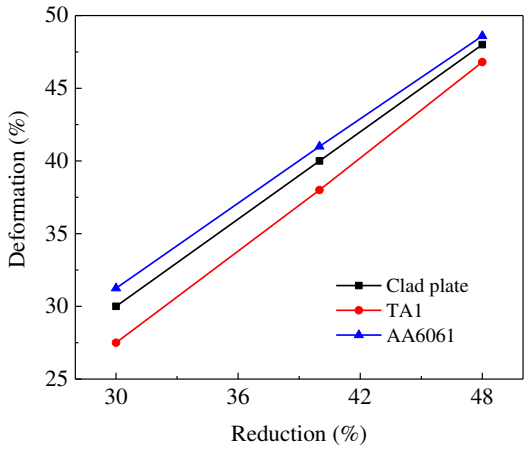

Fig.11 Deformation rate of Ti and Al with different reduction at 850 °C

Fig. 12 shows the interfacial bonding strength of Ti/Al laminated composites under the conditions of different rolling temperatures and different reductions. As can be seen from Fig. 12a, the interfacial bonding strength of the laminated composites obtained at a rolling temperature of 800 °C was higher than the composite plates prepared at 750 °C, while the interfacial bonding strength of the laminated composites decreased slightly to 800 °C. Comparing the bonding strength of titanium plates that were made at the rolling temperature of 800 °C with that of 850 °C, the variation of interfacial bonding strength of composite plate with the reduction is shown in Fig. 12b. The interfacial bonding strength of the laminated composites were basically consistent at the rolling temperature of 800 °C and 850 °C. When the reduction was less than 40%, the bonding strength increased approximately linearly as the reduction. When the reduction was greater than 40%, the increasing trend of the interfacial bonding strength slowed down. The bonding strength of the Ti/Al composite plate reached the peak value of 77MPa at 48% reduction and the rolling temperature of the titanium plate of 850 °C.

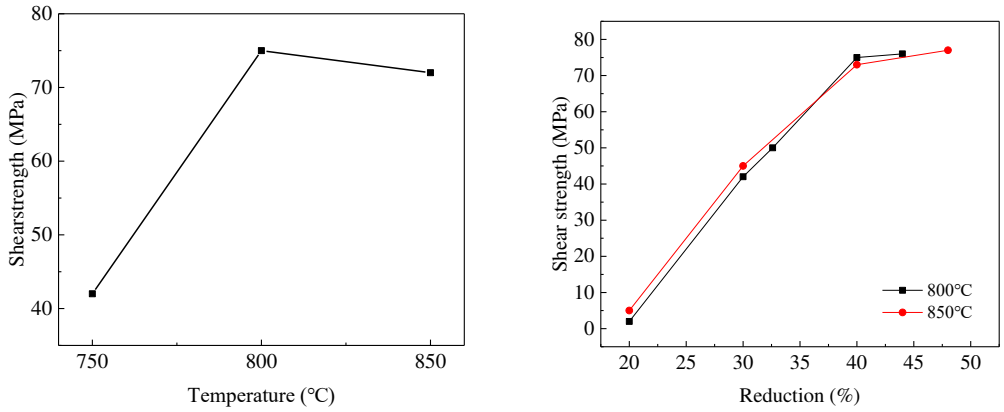

(a) effect of temperature on bonding strength

(b) effect of reduction on bonding strength.

Fig. 12 bonding strength of Composite board

Fig. 13 shows the results of SEM images and EDS line-scanning for Ti/Al composite interface under different processes. The results of line-scanning showed that the diffusion depth of two metal elements at the interface of Ti/Al composite plate were 1.286 μm, 1.400 μm, and 1.880 μm, respectively, at 30%, 40% and 48% reduction, deepening the diffusion of metal elements and improving the bonding strength of the interface. It can be seen from Fig. 13 that oxygen exists at the bonding interface, and its distribution at the interface decreased with the increase of the reduction. This is because oxidation was inevitable in rolling, and the presence of a metal oxide layer prevents the bonding of fresh metal. However, the increasing reduction can promote the tearing of the oxide layer on the metal surface, which formed solid metallurgical bonding of the fresh internal metal, thus improving the bonding strength. The SEM images and EDS surface-scanning of shear fracture on the titanium side are shown in Fig. 14. As shown in Fig. 14 a, b, and c, small cracks appeared on the fracture surface of the titanium plate, and the deformation resistance of the titanium side decreased with the increase of the rolling temperature of the titanium plate. The larger the deformation of the titanium plate relative to the aluminum plate, the wider and more cracks. With the increase of the reduction, the morphology of fracture surface on the titanium side changed, as shown in Fig. 14 c, d, and e. At 30% reduction, cracks appeared on the fracture surface, but the Al content was low, forming a small area of metallurgical bonding, which is called brittle fracture. At 40% reduction, dimples appeared on the fracture surface of the titanium side due to tensile-shear fracture. Compared with the condition of 30% reduction, more Al was bonded on the fracture surface of the titanium side, and thus the dimples had higher strength. Meanwhile, ductile fracture formed in the dimple area. At 48% reduction, a large area of Al remained on the fracture surface of the titanium side due to tensile-shear tests, as shown in Fig. 14f. EDS surface-scanning showed that the fracture surface of the titanium side was covered with Al by 83.1%. It is proved that Ti and Al formed a firm metallurgical bonding at this time, leading to the generation of fracture on the side of the aluminum substrate in the tension-shear test, and formed plastic fracture.

The results show that because of cracks on the surface of the Ti side in rolling and good

fluidity of aluminum, aluminum was squeezed into the cracks, causing the metallurgical bonding of two fresh metals under the action of pressure and high temperature. When the reduction amount increased, the larger the crack on the titanium side surface, the more metals were squeezed into the crack, and the higher the interfacial bonding strength. When sufficient metallurgical bonding of the two-metal formed at the bonding interface, due to the low tensile strength of Al, a large area of Al was bonded on the fracture surface on the titanium side in the tensile-shear process, and the bonding strength was almost equal to the shear strength of the Al substrate. The experimental results show that the Ti/Al differential temperature composite rolling could make the composite plates achieved high bonding strength, improving the coordination of deformation during preparation. Ti/Al differential temperature composite rolling, consequently, it can be regarded as an innovative method to fabricate Ti/Al composite plates using electromagnetic heating in Ti/Al differential temperature composite rolling.

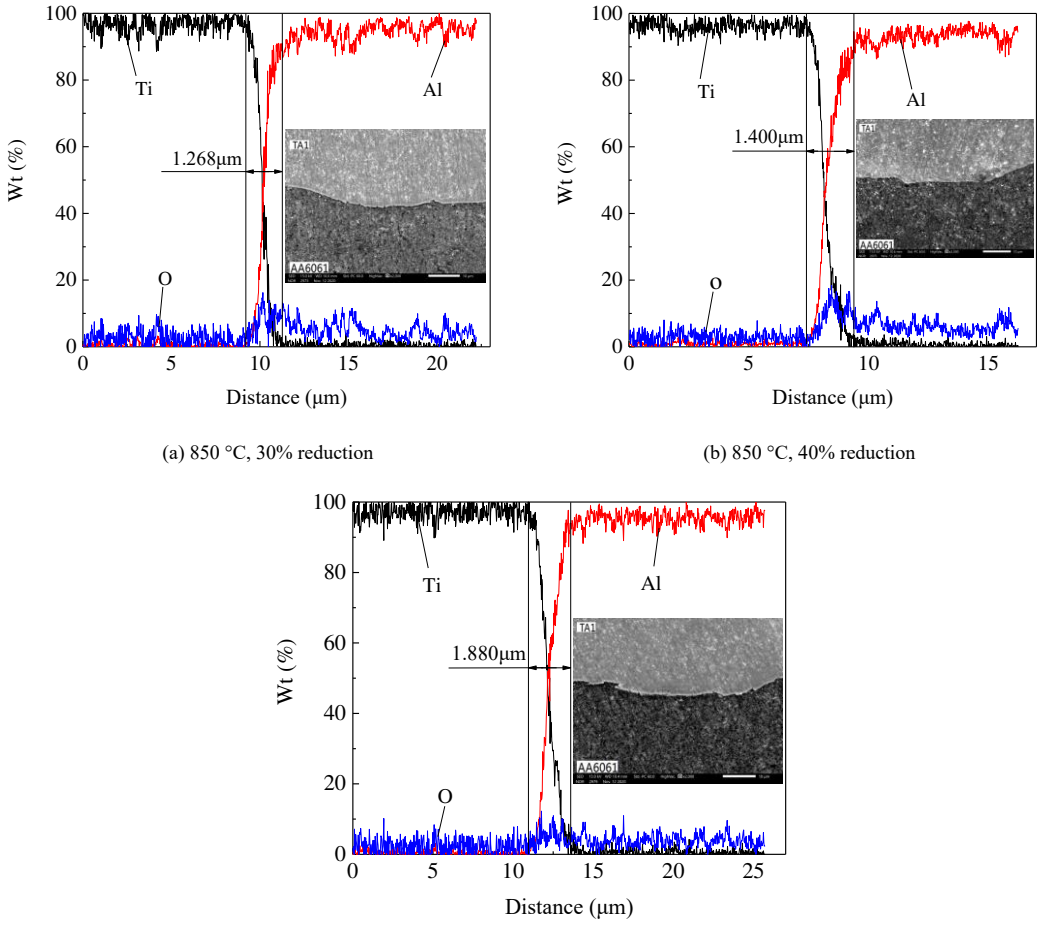

(a) 850 °C, 30% reduction

(b) 850 °C, 40% reduction

(c) 850 °C, 48% reduction

Fig. 13 Element line scanning and SEM images of Ti/Al composite interface

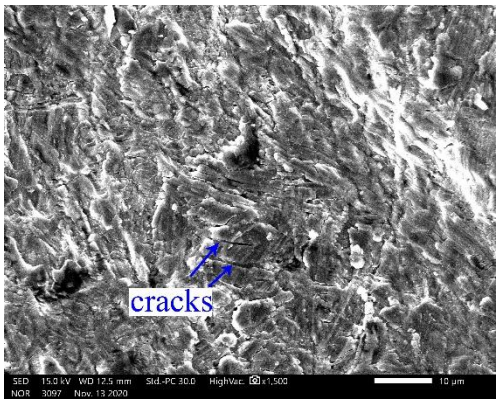

(a) 750 °C, 40% reduction

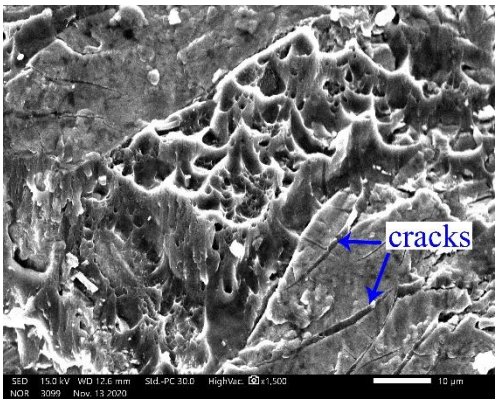

(b) 800 °C, 40% reduction

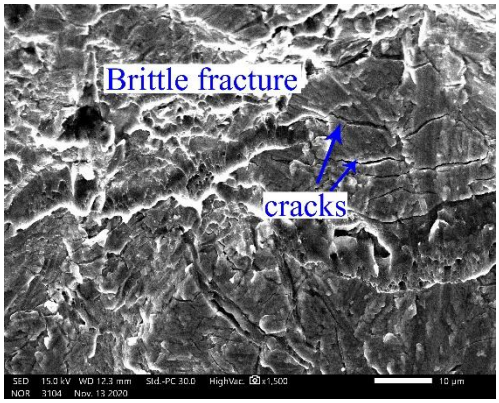

(c) 850 °C, 30% reduction

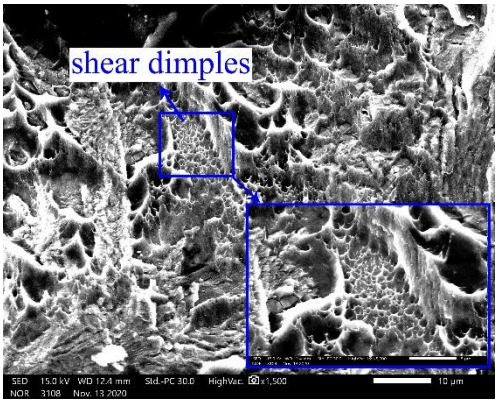

(d) 850 °C, 40% reduction

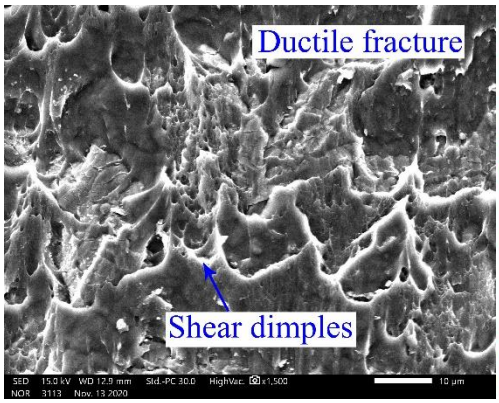

(e) 850 °C, 48% reduction

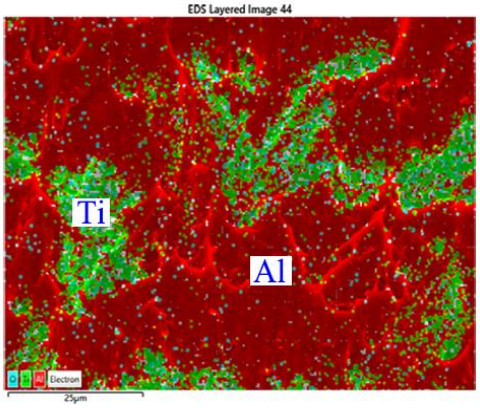

(f) element surface scanning of (e)

Fig. 14 SEM images of titanium side fracture

3 Conclusion

Using electromagnetic heating, the temperature difference of about 630 °C could be formed between the Ti plate and Al plate, and the temperature distribution of the two metal plates was relatively uniform, constructing the temperature field required by the Ti/Al homogeneous deformation bonding rolling.

(2) In the process of rolling, there would be an oxide layer at the bonding interface of the composite plate. The surface cracks became larger, as the deformation on the titanium side grew greater, which was more conducive to the squeezing of aluminum into the cracks, forming firm metallurgical bonding with fresh titanium under the action of pressure and high temperature.

(3) When the heating temperature of the titanium plate was 750-850 °C, and the reduction was 30%-48%, the deformation of the titanium plate and aluminum plate was more homogeneous with the increase of temperature of the titanium plate and reduction. The bonding strength of the Ti/Al composite plate reached 77MPa at the rolling temperature of titanium plate of 850 °C and the reduction of 48%.

Acknowledgments The authors would like to acknowledge the National Engineering Research Center for Equipment and Technology of Cold Rolled Strip.

Availability of data and material All data generated or analyzed during this study are included in this published article.

Authors' contributions Conceptualization: Chao Yu and Jirui Yu; Methodology: Chao Yu; Software: Chao Yu and Jirui Yu; Validation: Zhibin He, Qiang Lv and Jirui Yu; Formal analysis: Chao Yu and Zhibin He; Investigation: Chao Yu and Zhibin He; Resources: Zhibin He, Qiang Lv and Hong Xiao; Data curation: Zhibin He and Qiang Lv; Writing—original draft preparation: Chao Yu and Jirui Yu; Writing—review and editing: Chao Yu and Zhibin He; Visualization: Qiang Lv; Supervision: Hong Xiao; Project administration: Hong Xiao; Funding acquisition: Hong Xiao.

Funding The National Natural Science Foundation of China (52075472, 52004242), the National Key Research and Development Program (2018YFA0707302), and the Natural Science Foundation of Hebei Province (E2020203001)

Declarations

Ethics approval (include appropriate approvals or waivers) The manuscript has only communicated to one journal only. And has not submitted to more than one journal for simultaneous consideration.

Consent to participate The authors have given their consent to participate.

Consent for publication The authors have given their consent to publish the present paper.

Conflict of interest There is no conflicts of interest.

References

[1] Yang Y, Yu Y, Chen R (2020) A study on microstructural evolution and detwinning behavior of Ti–3Al–2.5V cold-rolled tube during annealing. Mater. Res. Express 7(9):096520.

[2] Ye XX, Tsec ZT, Tang GY, et al. (2015) Effect of electropulsing treatment on microstructure and mechanical properties of cold-rolled pure titanium strips. J. Mater. Process. Technol. 222:27−32.

[3] Jin HX, Wei KX, Li JM, et al. (2015) Research development of titanium alloy in aerospace industry. Chin. J. of Nonferrous Met. 25(2): 280−292.

[4] Altintas Y, Aksöz S, Keşlioğlu K (2015) Determination of thermodynamic properties of aluminum based binary and ternary alloys. J. Alloys Compd. 649:453-460.

[5] Huang GQ, Shen YF (2017) The effects of processing environments on the microstructure and mechanical properties of the Ti/5083Al composites produced by friction stir processing. J. Manuf. Process 30:361-373.

[6] Xiao H, Xu PP, Qi ZC, et al. (2020) Preparation of Steel/Aluminum Laminated Composites by Differential Temperature Rolling with Induction Heating. Acta Metall. Sin. 56(2);231-239.

[7] Xu SH, Zhou CS, Liu Y (2019) Research progress in metal-metal laminated structural composites. Chin. J. of Nonferrous Met. 29(6):1125-1142.

[8] Wang PJ, Chen ZJ, Huang HT, et al. (2020) Fabrication of Ti/Al/Mg laminated composites by hot roll bonding and their microstructures and mechanical properties. Chin. J. Aeronaut. 33(9):2281-2490 .

[9] Pei YB, Huang T, Chen FX, et al. (2020) Microstructure and fracture mechanism of Ti/Al layered composite fabricated by explosive welding. Vacuum 181.

[10] Huang HG, Chen P, Ji C (2017) Solid-liquid cast-rolling bonding (SLCRB) and annealing of Ti/Al cladding strip. Mater. Des. 118: 233-244.

[11] Mo T, Chen J, Chen Z, et al. (2019) Microstructure Evolution During Roll Bonding and Growth of Interfacial Intermetallic Compounds in Al/Ti/Al Laminated Metal Composites. JOM 71(12):4769–4777.

[12] Fan YM, Guo XZ, Cui SQ, et al. (2017) One-Step Explosive Bonding Preparation of Titanium/Aluminum/Titanium Laminates with Three Layers. Rare Met. Mater. Eng. 46(3):770-776.

[13] Qi ZC, Yu C, Xiao H, et al. (2018) Deformation coordination compatibility and bonding properties of Ti/Al composite plates prepared by different temperature rolling. Chin. J. of Nonferrous Met. 28(6):1120-1127.

[14] Li MQ, Jiang FL, Zhang H, et al. (2009) Deformation rule of steel/aluminum metal-laminate material during hot roll bonding. T. Nonferr. Metal. Soc 19(4):644.

[15] Han JC, Liu C, Jia D, et al. (2020) Research progress on titanium/aluminum composite plate. Chin. J. of Nonferrous Met. 30(6)：1270-1280.

[16] Peng LM，Li H，Wang JH (2005) Processing and mechanical behavior of laminated titanium-titanium tri-aluminide(Ti-Al3 Ti)composites. Mater. Sci. Eng.,A 406(1):309-318．

[17] Ma M, Huo P, Liu WC, et al. (2015) Microstructure and mechanical properties of Al/Ti/Al laminated composites prepared by roll bonding. Mater. Sci. Eng., A 636:301-310.

[18] Xiao H, Qi ZC, Yu C, et al. (2017) Preparation and properties for Ti/Al clad plates generated by differential temperature rolling. J. Mater. Process. Technol. 249:285-290.

[19] Qi ZC, Xiao H, Yu C, et al. (2019) Preparation, microstructure and mechanical properties of CP-Ti/AA6061-Al laminated composites by differential temperature rolling with induction heating. J. Manuf. Process. 44:133-144.

[20] Bao L, Wang B, You XP, et al. (2020) Numerical and experimental research on localized induction heating process for hot stamping steel sheets. Int. J. Heat Mass Transfer 151:119422.

Figures

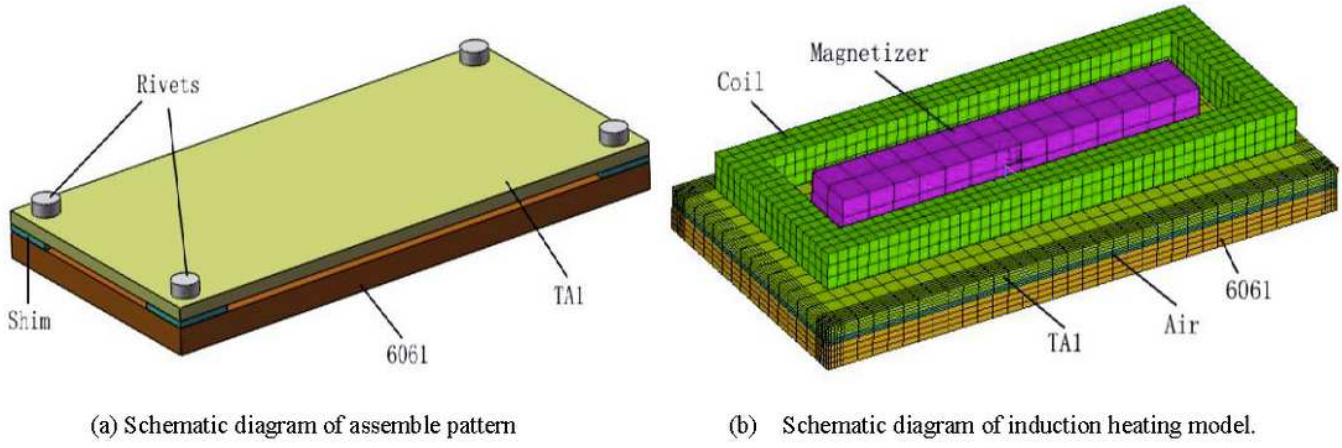

(a) Schematic diagram of assemble pattern (b) Schematic diagram of induction heating model.

Figure 1

Induction heating model

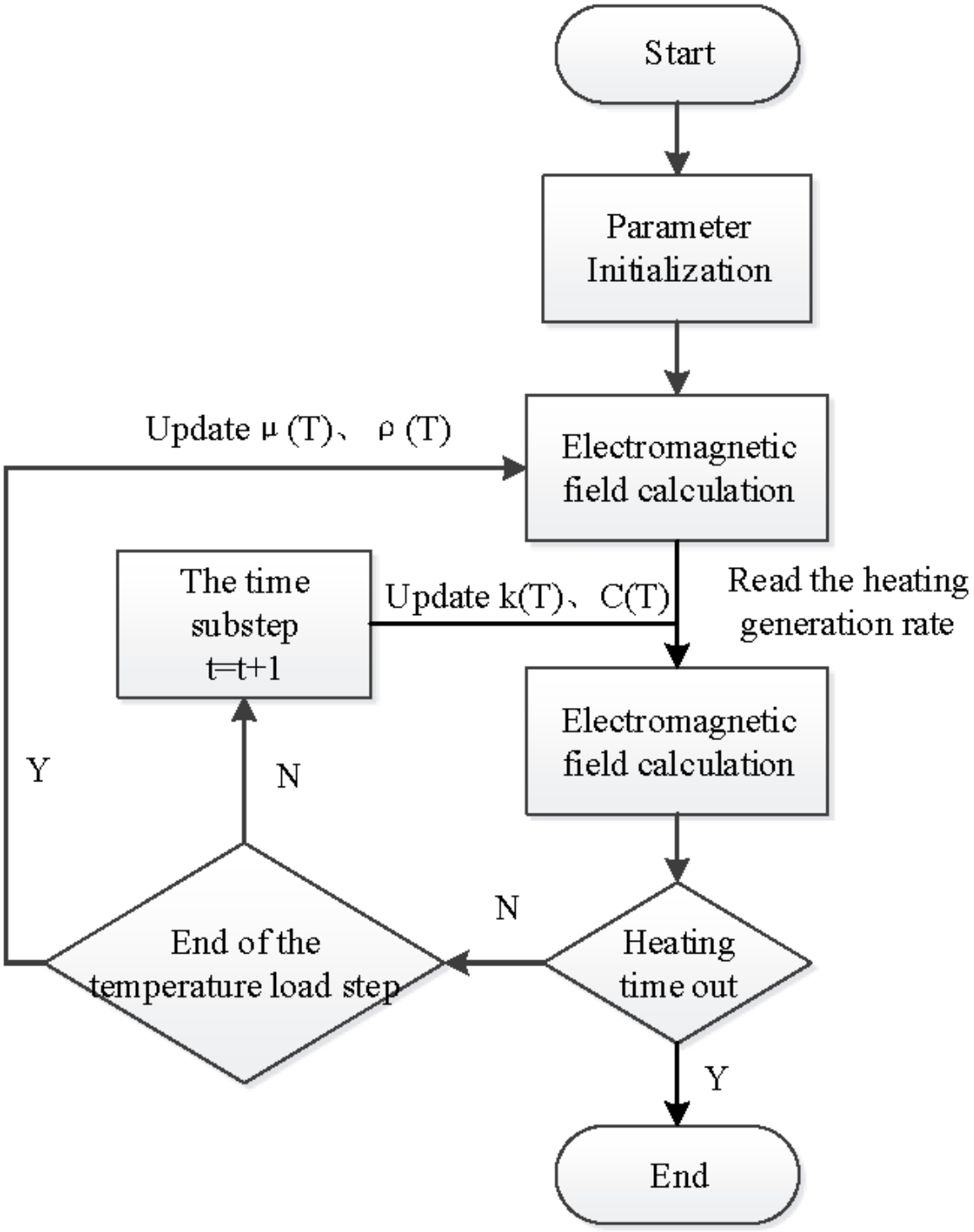

Figure 2

Flow chart of induction heating by finite element simulation

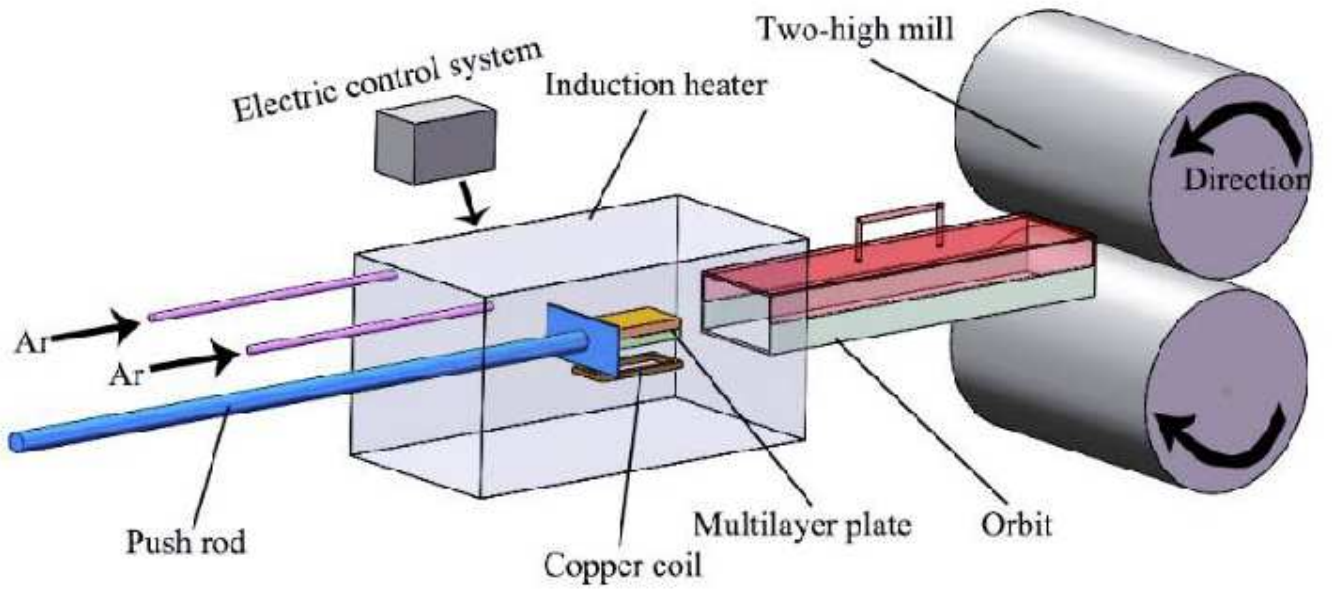

Figure 3

Schematic diagram of differential temperature rolling with induction heating method

Figure 4

Experimental platform

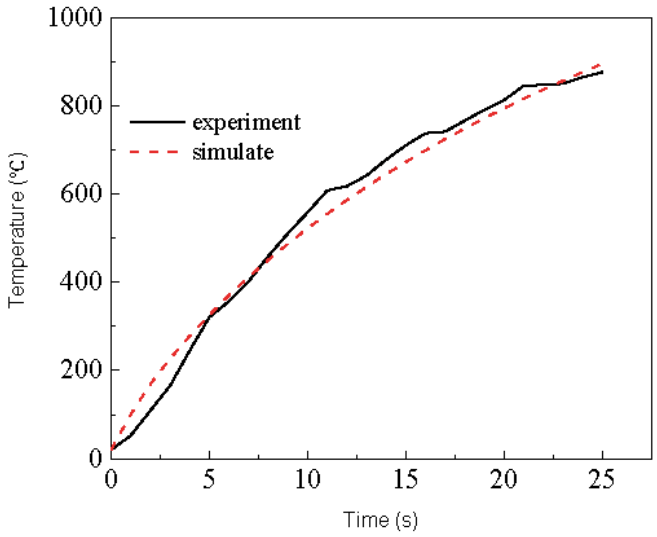

(a) Temperature of Ti plate

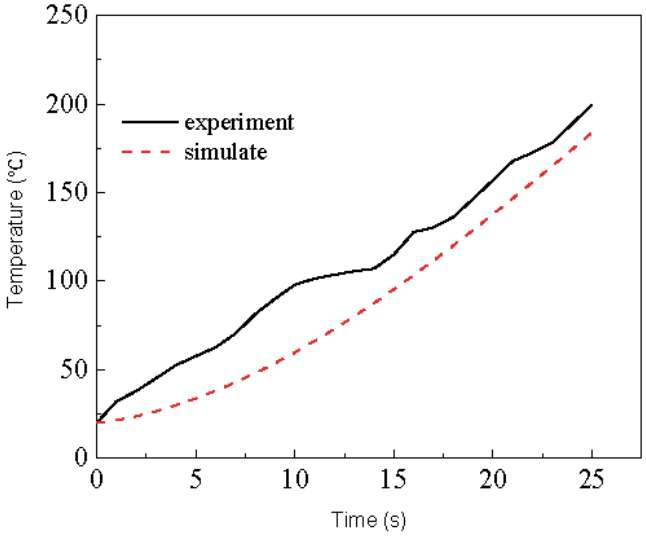

(b) Temperature of Al plate.

Figure 5

Temperature variation of the slab

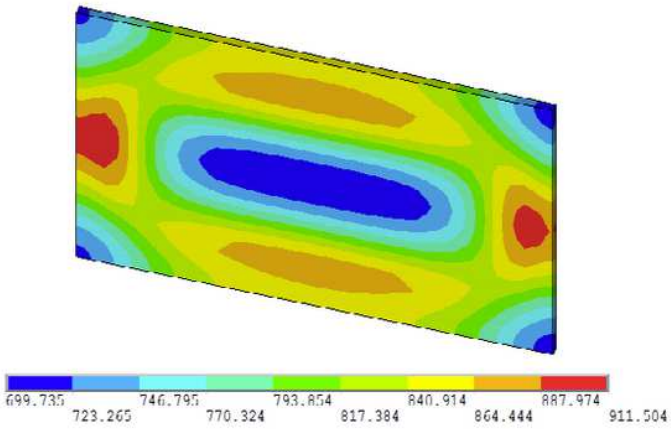

(a) cloud picture of the simulated Ti plate temperature

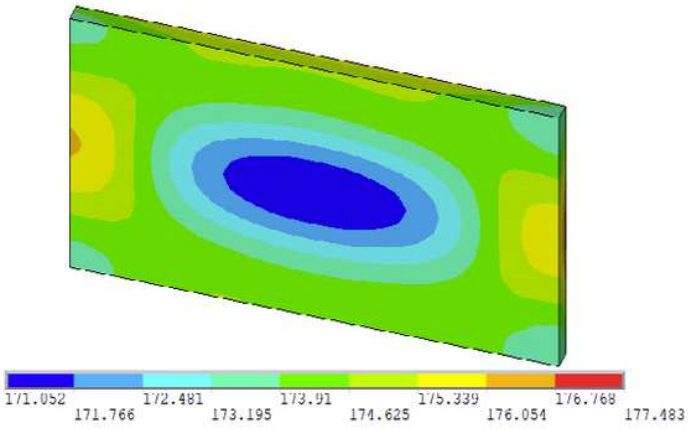

(b) cloud picture of the simulated Al plate temperature

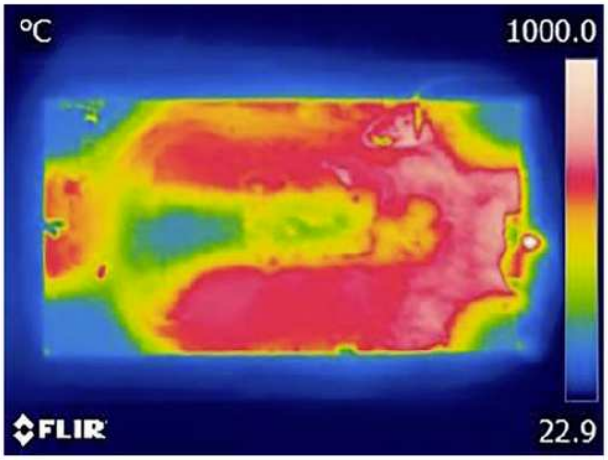

(c) cloud picture of the experimental Ti plate temperature distribution

Figure 6

Cloud picture of slab temperature distribution

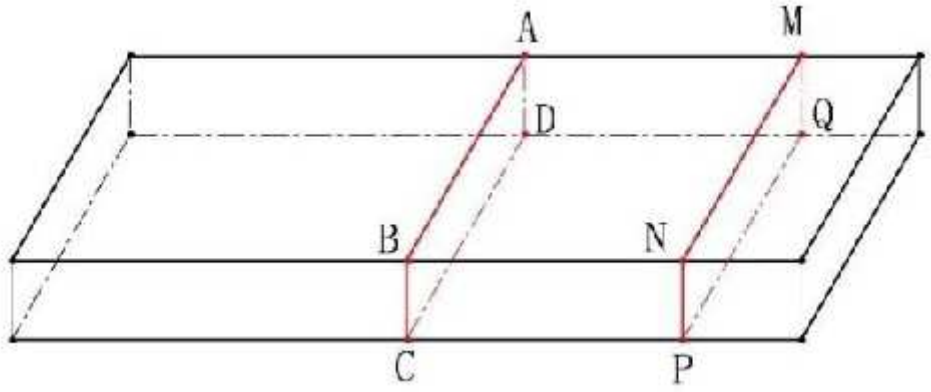

Figure 7

Position picture of the selected point of the slab

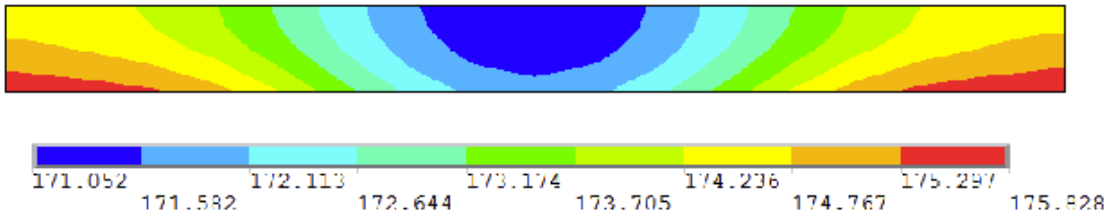

(a) Al plate cross-section of ABCD

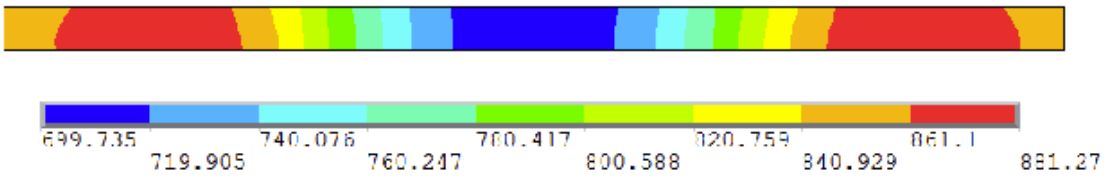

(b) Ti plate cross-section of ABCD

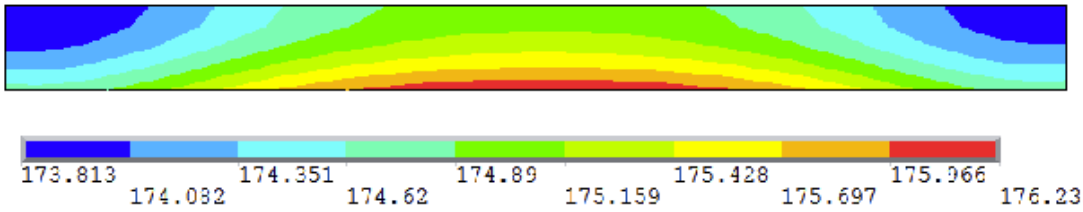

(c) Al plate cross-section of MNPQ

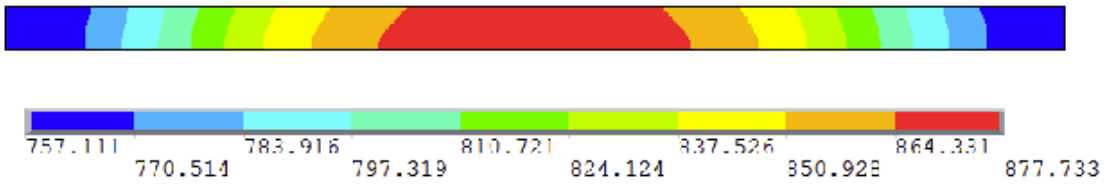

(d) Ti plate cross-section of MNPQ

Figure 8

Temperature field of slab cross-section

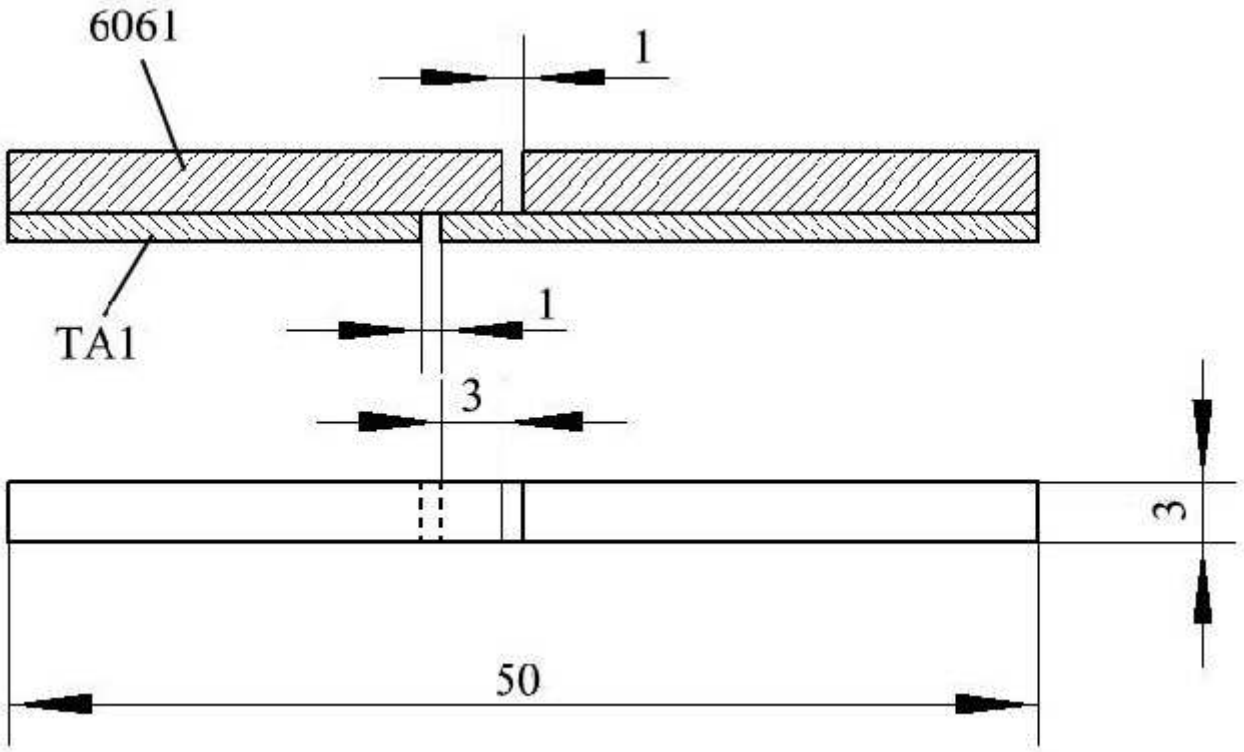

Figure 9

Tensile-shear specimen diagram

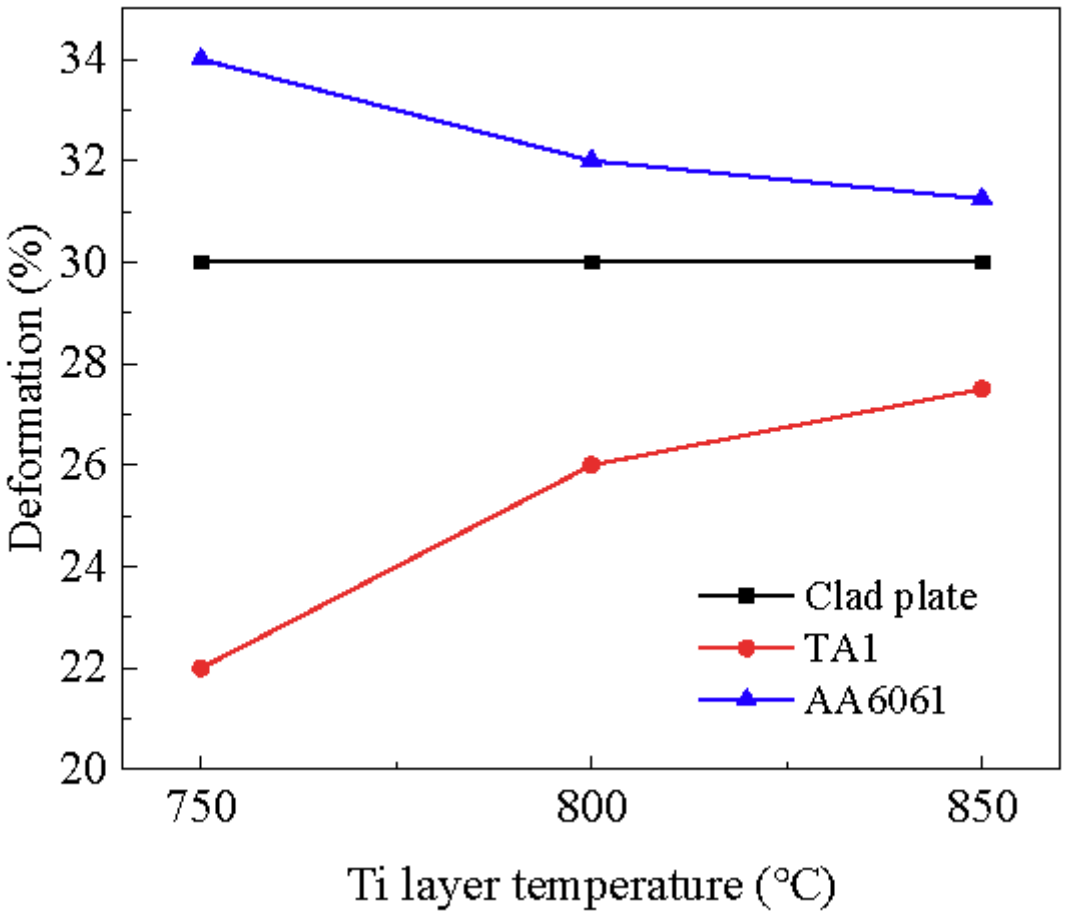

Figure 10

Deformation rate of Ti and Al with 30% reduction at different temperatures

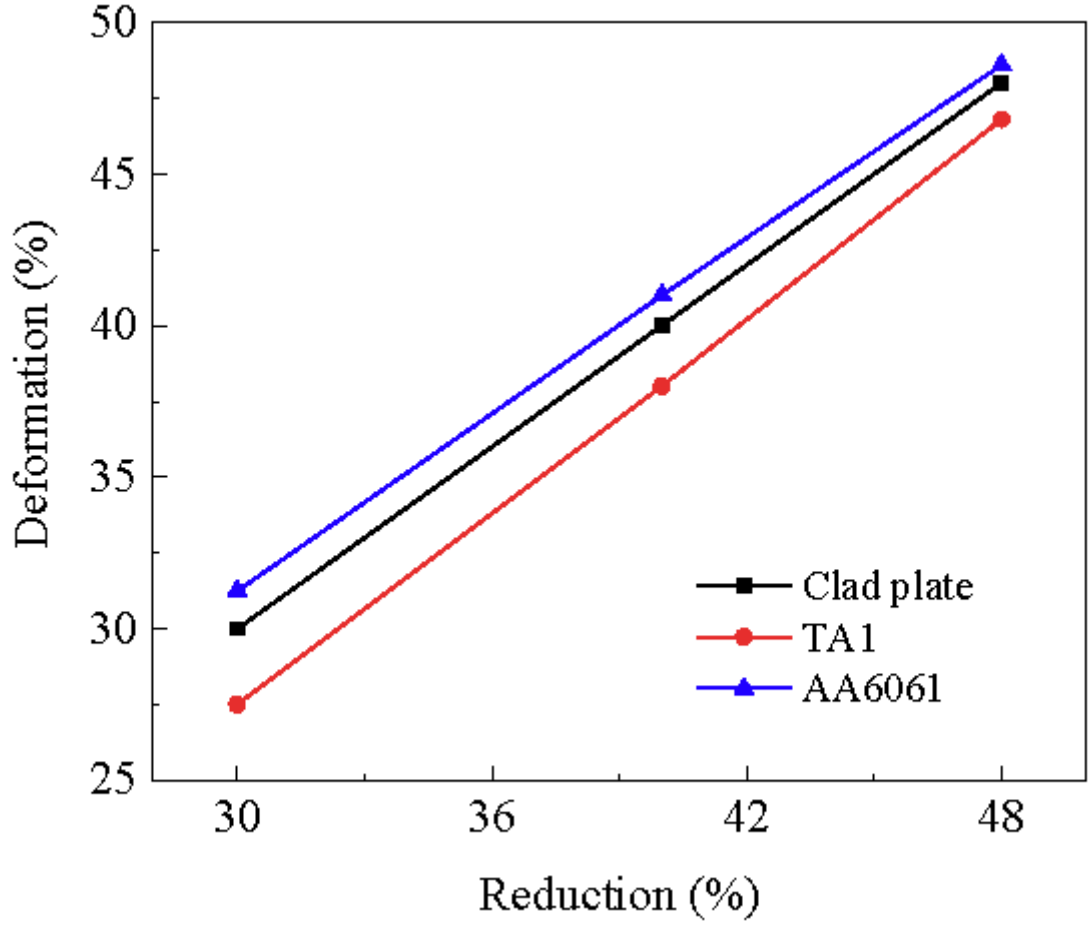

Figure 11

Deformation rate of Ti and Al with different reduction at 850 °C

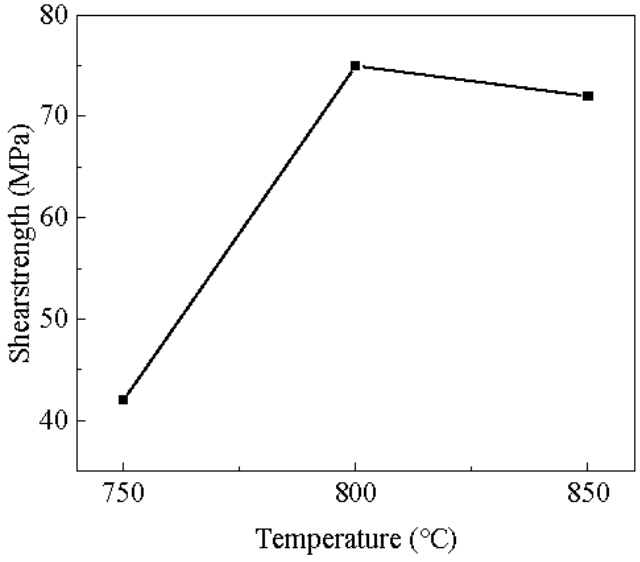

(a) effect of temperature on bonding strength

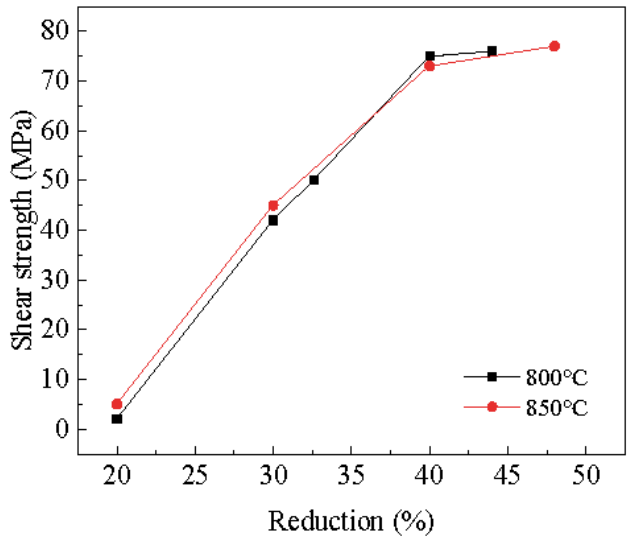

(b) effect of reduction on bonding strength.

Figure 12

bonding strength of Composite board

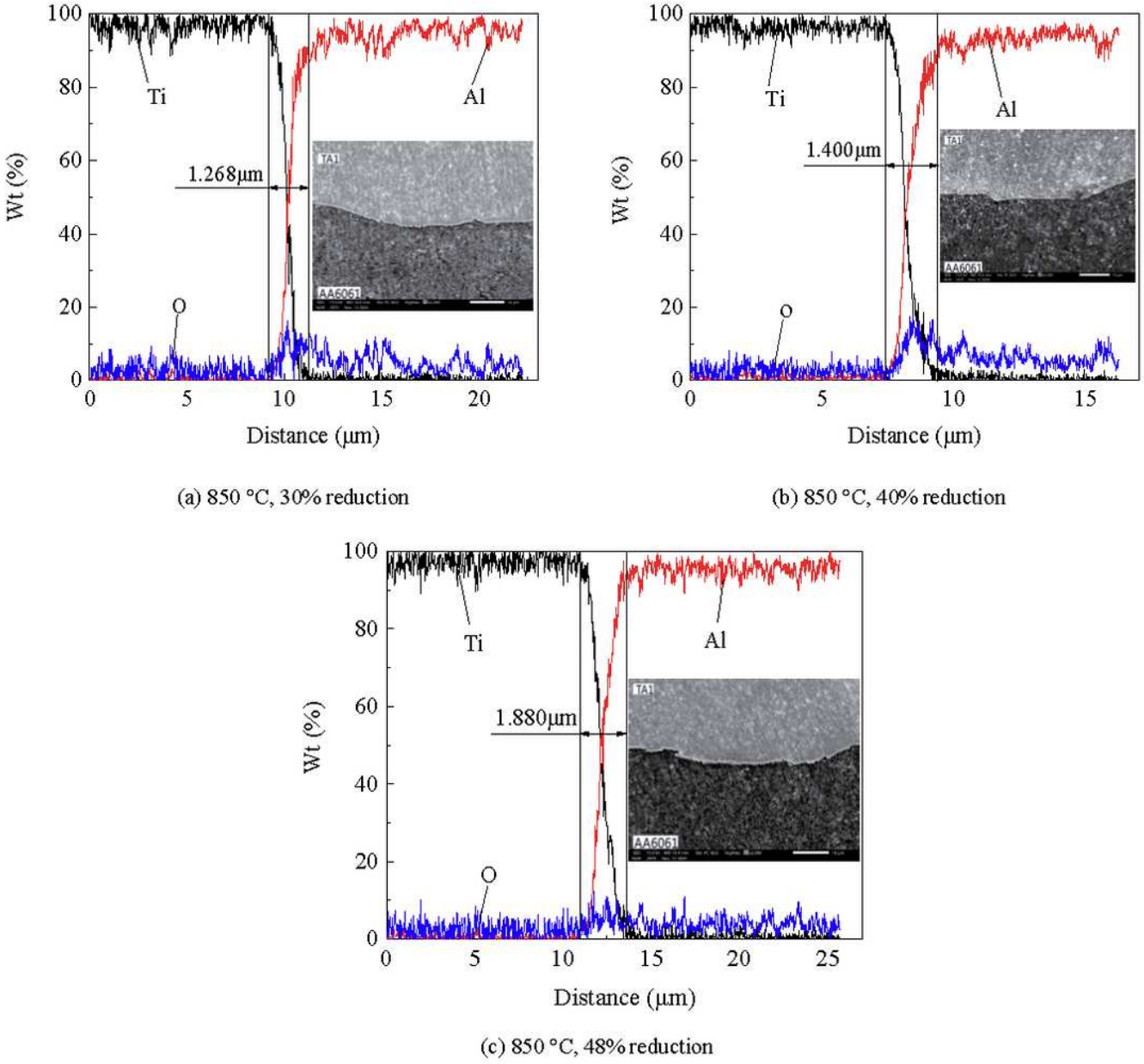

(a) 850 °C, 30% reduction

(b) 850 °C, 40% reduction

(c) 850 °C, 48% reduction

Figure 13

Element line scanning and SEM images of Ti/Al composite interface

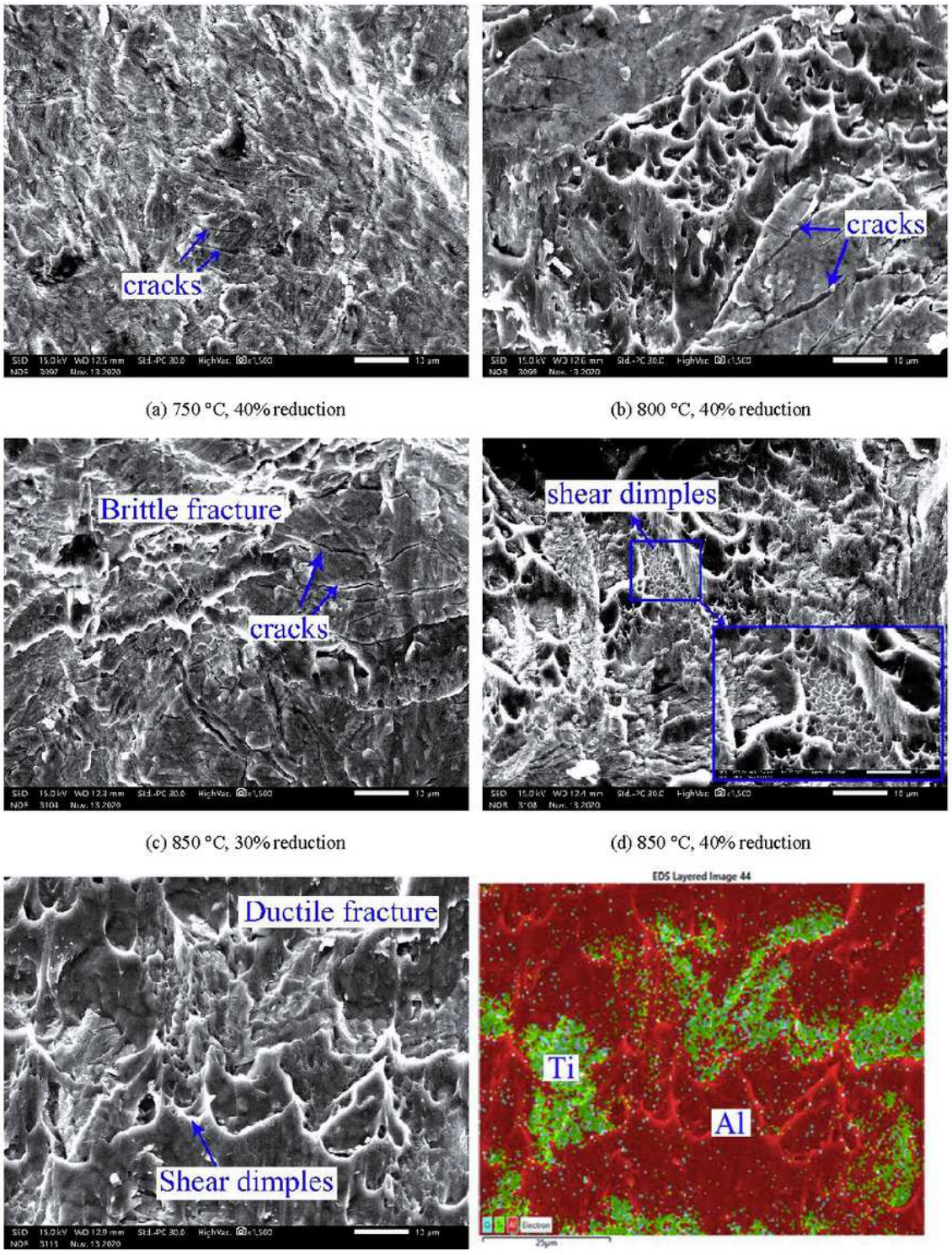

(a) 750 °C, 40% reduction

(b) 800 °C, 40% reduction

(c) 850 °C, 30% reduction

(d) 850 °C, 40% reduction

(e) 850 °C, 48% reduction

(f) element surface scanning of (e)

Figure 14

SEM images of titanium side fracture